VFAST Transactions on Mathematics
http://vfast.org/journals/index.php/VTM@ 2023, ISSN(e): 2309-0022, ISSN(p): 2411-6343
Volume 11, Number 1, January-June, 2023 *pp: 121-140*

MHD Flow and Heat Transfer of Micropolar Nanofluid on a Linearly Stretching/Shrinking Porous Surface

Sanjay Kumar[1*], **Asif Ali Shaikh**[1], **Hazoor Bux Lanjwani**[2*], **sayed feroz shah**[1]

[1*]Department of Basic Science and Related Studies, Mehran University of Engineering and Technology Jamshoro, Pakistan; [1]Department of Basic Science and Related Studies, Mehran University of Engineering and Technology Jamshoro, Pakistan; [2*]Institute of Mathematics and Computer Science, University of Sindh, 76080, Jamshoro, Pakistan

Keywords: *MHD, Heat source/sink, Micropolar nanofluid, Stretching and shrinking surfaces.*
Subject Classification: *MHD,Heat source,Mrcropolar nanofluid Modeling for nonlinear equation.*

Journal Info:
Submitted:
February 04, 2023
Accepted:
May 5, 2023
Published:
May 9, 2023

Abstract In this paper, there is considered incompressible steady two-dimensional laminar MHD boundary layer flow, heat and mass transfer characteristics of micropolar nanofluid on a linearly stretching/shrinking porous surface.The effects of the magnetic, thermal slip, mass slip and heat source sink parameters are also considered.By applying appropriate similarity variables,the system of governing partial differential equations associated to micropolar nanofluid flow is transformed into a system of non-linear ordinary differential equations.The resulting equations are numerically solved in the Maple software by using shooting technique.The impact of the different applied parameters on skin friction,couple stress, Nusselt and the Sherwood numbers along the related profiles are determined for both stretching ($\lambda > o$) and shrinking ($\lambda < 0$) cases of the surfaces.It was observed that with an increase in suction and magnetic parameters,the fluid velocity decreased. An increment in the thermal slip, the fluid temperature decreased and nanoparticles concentration decreases as the mass slip parameter is enhanced. An increase in concentration decreases but temperature increases. While, concentration and temperature both increase due to increase in thermophoresis parameter, and concentration also increases by increase in rate of chemical reaction. Thus, suction at the boundary and magnetic parameter acted as flow controlling parameter.It is believed that this type of investigation is very much helpful for the manufacturing of complex fluids and also for cleaning oil from surfaces.

***Correspondence Author Email Address:**
kumarsanjayarshi09@gmail.com

1 Introduction

The study of the non-Newtonian flowing fluid has acquired significant importance. Because of widely used fluids, such as water, paints, colloidal, additives, liquid crystal, biological fluids, and others, cannot entirely satisfy the characteristics of fluid flow in several industry sectors, Furthermore, the non-Newtonian fluid category contains a variety of complicated fluids, including Maxwell fluids, Casson fluids, micropolar fluids, etc. Eringen introduced one of the significant non-viscous fluids, which comprise micropolar fluid [13] .The micromotion of the fluid components and the microscopic effects exerted by the local structure are all taken into consideration in this hypothesis. According to the concept, a mathematical model for the behaviour of non-viscous fluids is included. This model can be used to study the actions of non-standard liquid crystals, polymers fluids, ferro-liquid, animal blood, lubricants, colloidal fluids, actual fluids with suspensions, and other fluids for which the Navier-Stokes theory is insufficient. The above microstructure particles contain various shapes and revolve separately from the fluid's motion [6].On the inclination plate, micropolar magnetohydrodynamic (MHD) fluid flow was examined by [7]. [11] also investigated the micropolar fluid flow using inclination surface with various physical characteristics. The entropic development of the micropolar flowing fluid over inclined channel using parallel plates was studied by [30]. [31] investigated micropolar fluid flow of heat exchange process while combining various fluid characteristics. [12] examined impact of Brownian motion, thermophoresis, and radiation over flow of micropolar Magnetohydrodynamic nanofluid over exponentially stretching and shrinking surfaces. [2] considered unsteady micropolar fluid flow, heat and mass transfer across curved stretching sheet. Additional relevant types of investigations on micropolar fluid from various aspects have been investigated in [1, 5, 17, 22].While, magnetohydrodynamic (MHD) is concerned to mathematical and physical scaffold that illustrates magnetic dynamics in fluid containing electricity. Magnetohydrodynamic has many usage in advanced manufacturing and other industries, which include films and drawing plastic wires, extruding polymers in the melting spinning processes, glass fiber production and crystal growth, manufacturing of foods and electronic chips, thermal energy storage, flow through filtering devices, fluid film in condensation processes, electrochemical processes and others. Several scholars have applied physical parameters to explore magnetohydrodynamic boundary layer flow across stretching and shrinking surfaces [3, 7, 8, 21, 26]. Additionally, since it has numerous uses in the medical and industrial sciences, nanotechnology has earned a great deal of interest from researchers. Industries employ carbon nanotube-infused graphite to produce lightest tennis racket, silver nano-particles to build storage containers particularly, zinc-oxide particles help shield items from UV light, and clay nano-composites to generate impermeable packaging films. Researchers in the biological sciences are constantly at work developing nano-capsules to replace injections which will pass through into stomach and into the bloodstream, while nano-particles' anti-bacterial abilities start making them suitable for bandage stitching and cutting. A subclass of that kind of emerging area is the nanofluid. These fluids are actually developed manufacturing fluids that are produced by suspending the nano scale particles (109–1011 m) in the typical traditional fluids. Since these fluids contain nanoparticles, [10] called these fluids "nanofluids." In the last few years different engineering problems which have already been researched by many investigators on the advancement of nanofluids [18, 23]. Using two phase nanofluid model Buongiorno [24] studied the extensive convection of heat transfers in nanofluids. In addition, researchers [20, 29] have discussed the fluid flow of nanofluids over stretching and shrinking surfaces, because of its huge prospects for use in engineering and technological applications.[28] considered the nanofluid flow at the stagnation point. Free convective boundary layer flow of the nanofluid over

vertically moving plate was put into consideration by [19]. While, [9] applied the [24] Model to study magnetohydrodynamics mixed convective nanofluid flow including buoyancy effects. The natural convection flow of nanofluid with magnetic parameter on a stretching vertical sheet was considered by [14, 27].[16] considered characteristics of rate of heat transfer of the nanofluid in permeable media and have showed natural convection in the nanofluid flow between two triangular entrapped cavities with effects of thermophoresis diffusions and Brownian applying method of finite difference. Motivated from above cited literature, there are considered two dimensional laminar magnetohydrodynamic boundary layer flow of micropolar nanofluid on linearly stretching/shrinking surface with heat source sink parameter, magnetic, concentration slip, thermal slip, Brownian motion and thermophoretic impacts .To modify the equations, Buongiorno model is considered in porous medium. Here, we have extended the work done by [4].To best of the author's knowledge, such attempt on the MHD boundary layer micropolar nanofluid in existence of heat source sink, magnetic field, thermal and concentration slips parameters on the linearly stretching and shrinking surfaces have not been examined earlier. The acquired results are graphically displayed and discussed in detail. The present investigation is expected to be useful for new researchers who are interested in examining the influence of different parameters on boundary layer flow of micropolar nanofluid across stretching/shrinking surface at a time.

2 Problem formulation

Consider two-dimensional laminar steady MHD boundary layer flow of chemical reacting micropolar nanofluid on the linearly stretching/shrinking surface to porous medium under thermal and mass slip effects in the coordinate system (x, y). Where y-axis is considered perpendicular to surface and flow is considered along the x-axis that is displayed in the Figure 1.

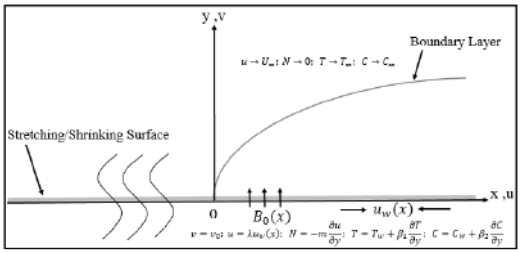

Figure 1. Flow model and the coordinate system.

$$\frac{\partial u}{\partial x} + \frac{\partial v}{\partial y} = 0 \tag{1}$$

$$u\frac{\partial u}{\partial x} + v\frac{\partial u}{\partial y} = \left(\vartheta + \frac{K_1}{\rho}\right)\frac{\partial^2 u}{\partial y^2} + \frac{K_1}{\rho}\frac{\partial N}{\partial y} - \frac{\sigma B_0^2(x)u}{\rho} \tag{2}$$

$$u\frac{\partial N}{\partial x} + v\frac{\partial N}{\partial y} = \frac{1}{\rho j}\left[\gamma^*\frac{\partial^2 N}{\partial y^2} - K_1\left(2N + \frac{\partial u}{\partial y}\right)\right] \tag{3}$$

$$u\frac{\partial T}{\partial x} + v\frac{\partial T}{\partial y} = \alpha\frac{\partial^2 T}{\partial y^2} + \tau_w\left[D_B\frac{\partial C}{\partial y}\frac{\partial T}{\partial y} + \frac{D_T}{T_\infty}\left(\frac{\partial T}{\partial y}\right)^2\right] + \frac{Q_0}{\rho c_p}(T - T_\infty) \tag{4}$$

$$u\frac{\partial C}{\partial x} + v\frac{\partial C}{\partial y} = D_B\frac{\partial^2 C}{\partial y^2} + \frac{D_T}{T_\infty}\frac{\partial^2 T}{\partial y^2} - K^*(T - T_\infty) \tag{5}$$

Subject to boundary conditions

$$\begin{gathered} v = v_w(x); \quad u = a\lambda x; N = -m\frac{\partial u}{\partial y}; T = T_w + \beta_1\frac{\partial T}{\partial y}; C = C_w + \beta_2\frac{\partial C}{\partial y} \text{ at } y = 0, \\ u \to 0; N \to 0; T \to T_m; C \to C_m \text{ as } v \to \infty \end{gathered} \tag{6}$$

Uniform magnetized field with B_0 strength is used to transverse to linearly stretched surface, invoking a Lorentz magneting body force with plane surface. The surface shrinks and stretches linearly with $U_w = ax$ velocity, here $a > 0$ Shows constant of stretching. Where, a viscous dissipation and heat source is considered. Also, the first ordered similar chemical reaction is taken into account. Eringen's micropolar model of micro-structural rheological features with Buongiorno's model is applied for nanofluid flow. Following to the mentioned assumptions, continuity, momentum, angular momentum, energy and concentration equations are written as:

Here, u and v represents velocity components in respective of x and y-axes. Electrical conductivity and kinematic viscosity are denoted by σ and ϑ, respectively. Density of fluid and specific heat with constant pressure are denoted by ρ and c_p respectively. $B_o(x)$ is constant of magnetic field. γ^* denotes spin gradient's viscosity, N denotes micro rotation, j is ratio between micro-inertia and mass unit and k_1 is vortex viscosity, α stands for thermal diffusivity and k indicates thermal conductivity of fluid. The m is constant and its range is $0 \leq m \leq 1$. We obtain N = 0 when m = 0, that denote stronger concentration, bringing the micro particles nearer to surface in which they are unable to revolve.Moreover, when m = $\frac{1}{2}$ that exhibits a weak concentration, it may cause anti-symmetric part of the stress tensor to be vanished. In the boundary layer flows modelling,m = 1 indicates turbulence [15]. In addition, several researchers assumed $\gamma^* = (\mu + \frac{k_1}{2})j = \mu \times (1 + \frac{k}{2})j$ C is nanoparticles volumetric fractions, T is temperature, T_∞ is ambient fluid temperature, T_w is surface temperature and $K_1 = \mu K$ is material parameter, D_B and D_T are Brownian and thermophoresis diffusions coefficients respectively. Furthermore, following linear type of the similarity transformation are used to get the similarity solutions.

$$\begin{gathered} \eta = y\sqrt{\frac{a}{\vartheta}}, u = axf'(\eta), v = -\sqrt{a\vartheta}f(\eta), N = \sqrt{\frac{a}{\vartheta}}axg(\eta), \\ \theta(\eta) = \frac{(T-T_\infty)}{(T_w - T_\infty)}, \quad \emptyset(\eta) = \frac{(C-C_\infty)}{(C_w - C_\infty)}, \end{gathered} \tag{7}$$

where $\psi = \sqrt{a\vartheta}xf(\eta)$, is a stream function the continuity equation is obviously satisfied the ordinary diffrential equations of following to dimensionless form ae achived by applying equation (7) in equation (2) to (6);

$$(1 + K)f''' + ff'' - f'^2 + Kg' - Mf' = 0, \tag{8}$$

$$\left(1 + \frac{K}{2}\right)g'' + fg' - gf' - 2Kg - Kf'' = 0, \tag{9}$$

$$\frac{1}{Pr}\theta'' + f\theta' + Nb\emptyset'\theta' + Nt(\theta')^2 + Q\theta = 0, \tag{10}$$

$$\phi'' + Lef\phi' + \frac{Nt}{Nb}\theta'' - Le.\varepsilon\phi = 0. \tag{11}$$

Boundary conditions take the form:

$$\begin{gathered} f(0) = S, f'(0) = \lambda, g(0) = -mf''(0), \theta(0) = 1 + \delta_T\theta'(0), \phi(0) = 1 + \delta_c\phi'(0); \\ f'(\eta) \to 0, g(n) \to 0, \theta(\eta) \to 0, \phi(\eta) \to 0 as \eta \to \infty \end{gathered} \tag{12}$$

where, prime express derivative with respect to η, Pr = $\frac{\vartheta}{\alpha}$ is a Prandtl number K = $\frac{k}{\mu}$ indecates micropolar material parameter, N_t = $\frac{\tau_w D_T (T_w - T_\infty)}{\vartheta T_\theta}$ is therophoresis parameter, N_b = $\frac{T_w D_B (C_w - C_\infty)}{\vartheta}$ is a Brownian motion parameter, and Le = $\frac{\vartheta}{D_B}$ is Lewish number, moreover,S = $-\frac{v_0}{\sqrt{a\vartheta}}$ is the suction parameter ($S > 0$), $\epsilon = \frac{K^*}{a}$ is the chemical reaction parameter, $\delta_T = \beta_1 \sqrt{\frac{a}{\vartheta}}$ is the thermal slip and $\delta_c = \beta_2 \sqrt{\frac{a}{\vartheta}}$ is the concentration Slip parameters, $Q = \frac{Q_0}{a \rho c_p}$ is the heat source/ Sink parameter.

3 Physical Quantities of the Engineering Intrest

The significant physical quantities of interests are skin friction coefficient C_f,couple stress C_S, Nusselt number (Nu_x), and the Sherwood number (Sh_x).These quantities are significant for process of materials procedures. These assume the given form as:

$$C_f = \frac{\left[(\mu + \kappa)\frac{\partial u}{\partial y} + \kappa N\right]_{y=0}}{\rho u_w^2}, \quad C_s = \left[\frac{\vartheta}{a}\frac{\partial N}{\partial y}\right]_{y=0}, \; Nu_x = \frac{-x\left[\frac{\partial T}{\partial y}\right]_{y=0}}{(T_w - T_\infty)}, \; Sh_x = \frac{-x\left(\frac{\partial C}{\partial y}\right)_{y=0}}{(C_w - C_\infty)} \tag{13}$$

Using equation (7) in (13), we get:

$$C_f (Re_x)^{\frac{1}{2}} = (1 + (1-m)K) f''(0), \quad C_s = (1 + K/2) g'(0), \; N_u (Re_x)^{-\frac{1}{2}} = -\theta'(0), \quad Sh_x (Re_x)^{-\frac{1}{2}} = -\emptyset'(0), \tag{14}$$

Where $Re_x = \frac{ax^2}{\vartheta}$ is local Reynolds number.

4 NUmerical Methodology

The boundary value problem mentioned in the equations (8)-(11) associated to boundary conditions (12) has been tackled by shooting method [25]. Boundary values problems (BVPs) are changed into initial values problems (IVPs) with help of shooting method. Thus, there is obtained:

$$f' = F_P, \; f'' = F_{PP}, (1 + K) F'_{PP} + F F_{PP} - (F_P)^2 + K G_P - M f' = 0 \tag{15}$$

$$g' = G_P, \; \left(1 + \frac{K}{2}\right) G'_P + F G_P - G F_P - 2KG - K F_{PP} = 0 \tag{16}$$

$$\theta' = \theta_P, \phi' = \phi_P, \; \frac{1}{Pr}\theta'_P + F\theta_P + N_b \phi_P \theta_P + N_t (\theta_P)^2 = 0 \tag{17}$$

$$\phi' = \phi_P, \phi'_P + LeF\phi_P + \frac{N_t}{N_b}\theta'_P - Le.\varepsilon\phi = 0 \tag{18}$$

Subject to boundary conditions:

$$\begin{aligned} F(0) = S, F_P(0) = \lambda, \quad & F_{PP}(0) = \alpha_1, \\ G(0) = -m\alpha_1, \quad & G_P(0) = \alpha_2, \\ \theta_P = 1 + \delta_T \alpha_3, \quad & \theta_P(0) = \alpha_3, \\ \phi(0) = 1 + \delta_C \alpha_4, \quad & \phi_P(0) = \alpha_4, \end{aligned} \tag{19}$$

Here, the missing initial conditions are denoted as$\alpha_1, \alpha_2, \alpha_3$ and α_4. The missing values of $\alpha_1, \alpha_2, \alpha_3$ and α_4 are crucial and may be selected carefully which may satisfy given boundary conditions mentioned in equation (12). Using the Maple program with the help of the shootlib function, computations are carried out in this problem [25].

5 Result and Discussion

Numerical computation of equations (8)-(11) subject to boundary conditions specified in equations (12) are obtained in Maple software using shooting method. The impacts of the different physical flow parameters on the skin friction coefficients $f''(0)$, couple stress $g'(0)$, Nusselt number $-\theta'(0)$ and the Sherwood number $\phi'(0)$,are determined and presented graphically in Figures 2-26. Some of our acquired results are compared with results mentioned in previous research by Afify, [26] in order to validate our computed results. The comparison demonstrates the excellent resemblance that has been presented in Table 1. Moreover, numerical computations are carried out to explain velocity, angular velocity, heat and nanoparticles concentration profiles. The effects of obtained results of used parameters on different profiles are represented. Where, Figure 2-5 shows the variation of skin friction coefficient $f''(0)$, couple stress $g'(0)$, Nusselt number $-\theta'(0)$ and Sherwood number $\phi'(0)$ along λ at various values of suction parameter S.

Pr	λ	Afify[26]	Present
0.07	1.0	0.0662	0.0663
0.20		0.1691	0.1689
0.70		0.4538	0.4539
2.0		0.91113	0.9113
0.7		1.8954	1.8953

Table 1. Comparison of $-\theta(0)$ for different values of the Pr when M = Nb = Nt = Q = ϵ = Le = δ_T = δ_C = 0

There is examined from figure 2-3 that rate of skin friction and couple stress declines for stretching surface $\lambda > 0$ and rises for shrinking surface $\lambda < 0$ when suction parameter is increased. While, Figures 4 and 5 show an increase in Nusselt and Sherwood numbers for shrinking and stretching cases of surfaces as rate of the suction is increased, respectively.

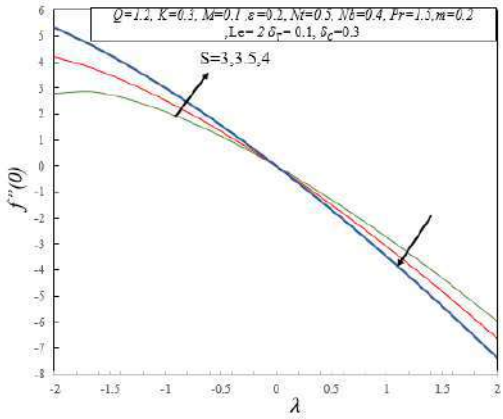

Figure 2. The variation of skin friction coefficient along λ at various values of suction parameter S.

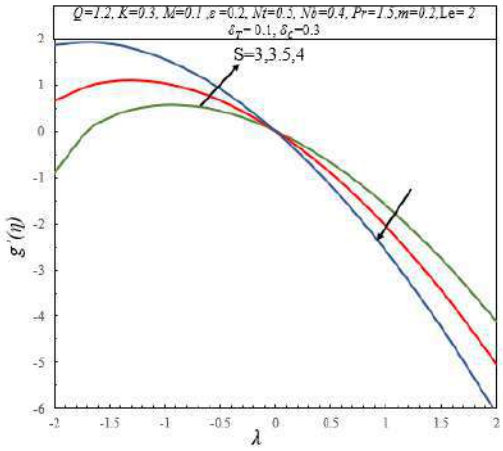

Figure 3. The variation in couple stress $g'(0)$ along λ at various values of S

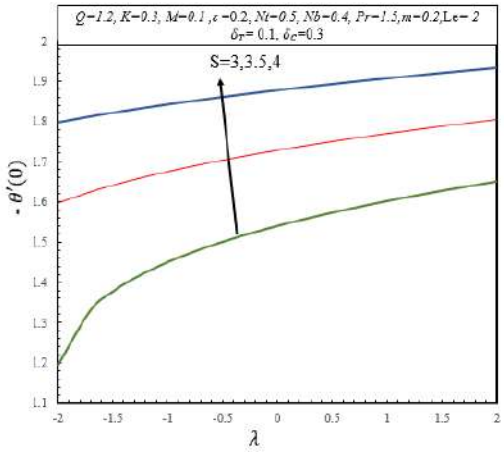

Figure 4. The variation in Nusselt number along λ at various values S.

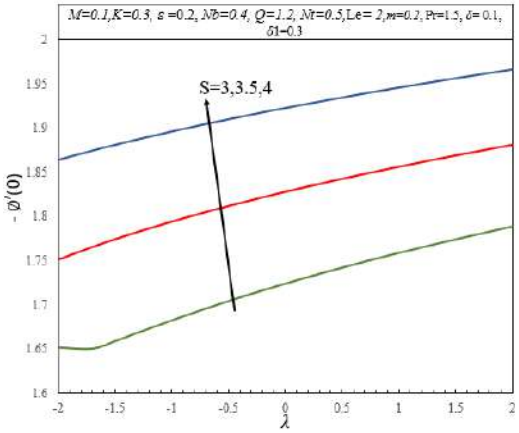

Figure 5. The variation in Sherwood Number along λ at various values S

Figures 6-7 depicts impacts on velocity and angular velocity profiles due to variation of magnetic parameter M. The magnetic field generates the Lorentz force that resists the momentum of particles of fluid. Figure 6 shows due to Lorentz force that causes the velocity boundary layer shift towards direction of the surface. Figure 7 demonstrated that as the values of magnetic parameter enhances, the angular velocity profile and its boundary layer thickness rises. The Lorentz force, which slows down fluid velocity, is primarily to responsible for the decrease in the angular velocity profile. Figure 8-11 show influence on velocity f angular velocity profile $g(\eta)$, temperature $\theta(\eta)$ and concentration $\phi(\eta)$ due to variation of suction parameter S. There are observed the velocity, temperature and the concentration profiles along thicknesses of their boundary layers are decreasing with increase in rate of the suction S for both cases of surfaces. While at the start angular velocity of micro-polar nano-fluid increases but after a point it decreases throughout the flow.

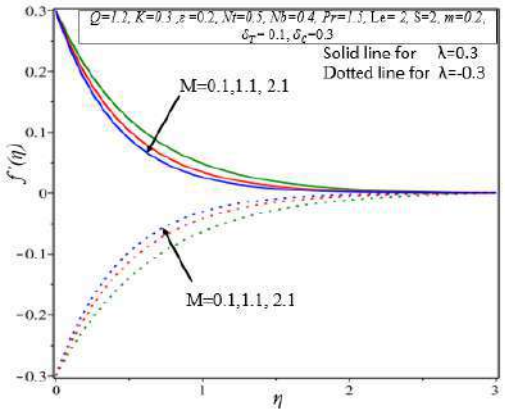

Figure 6. Influence of M on velocity profile f′(η)

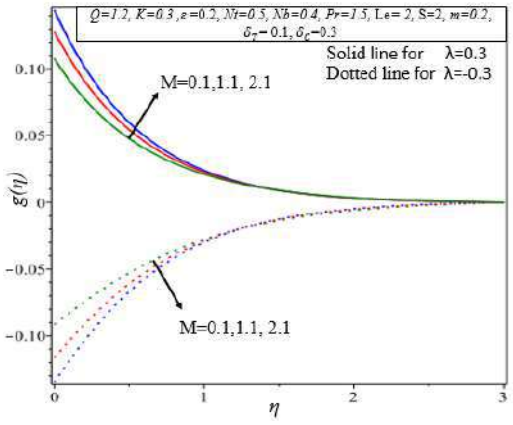

Figure 7. Influence of S on the angular velocity profile g(η)

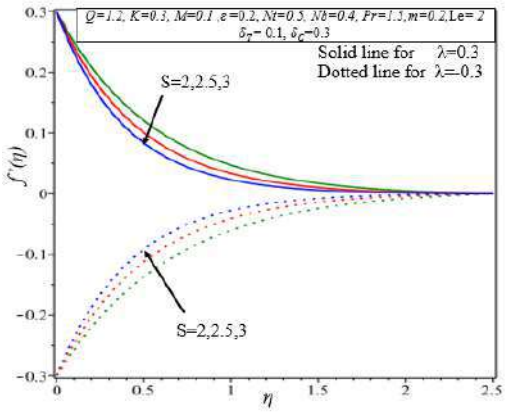

Figure 8. Influence of S on the velocity profile $f'(\eta)$

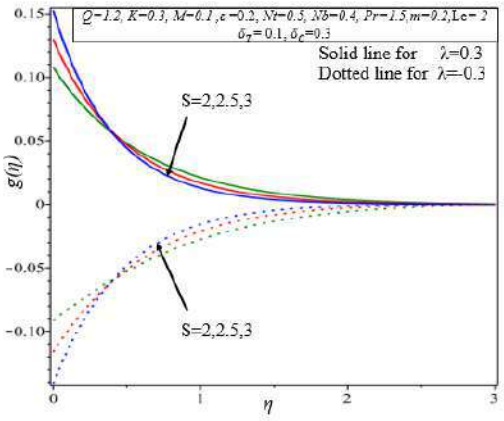

Figure 9. Influence of S on the angular velocity profile $g(\eta)$

Figures 12 -13 exhibit the influence on temperature profile $\theta(\eta)$ due to increment in the Brownian motion parameter (*Nb*) and thermophoresis parameter (*Nt*) respectively. It has been observed that temperature profile along with thermal boundary layer thickness rise due to any increment in Brownian motion and thermophoresis parameters. Due to increment in(*Nb*)and (*Nt*) the rate of temperature gradient at the surfaces are enhanced. Figures 14 - 15 show effect on concentration profiles $\phi(\eta)$ for increasing rate of Brownian motion parameter and thermophoresis parameter. Figure 14 demonstrates that concentration of nanoparticles in the micropolar nanofluid decreases as (*Nb*) concentration rises throughout the flow. Figure 15 illustrates that as (*Nb*) is enhances both temperature and thickness of its boundary layer when it is raised. This is because of Brownian motion, in which particles flow with increasing kinetic energy in a "zig-zag" pattern, causes more particles collisions. The concentration and the corresponding boundary layer thickness decrease for stretching as well as shrinking surfaces as (*Nb*) increases.

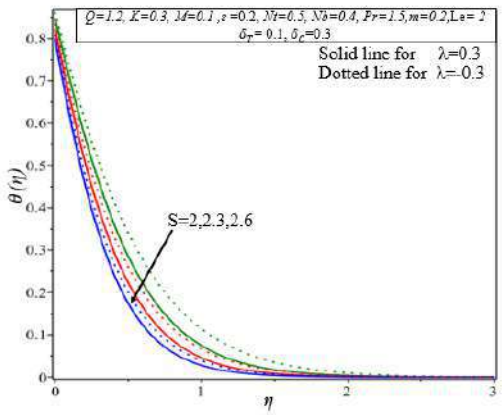

Figure 10. Influence of S on the temperature profile $\theta(\eta)$

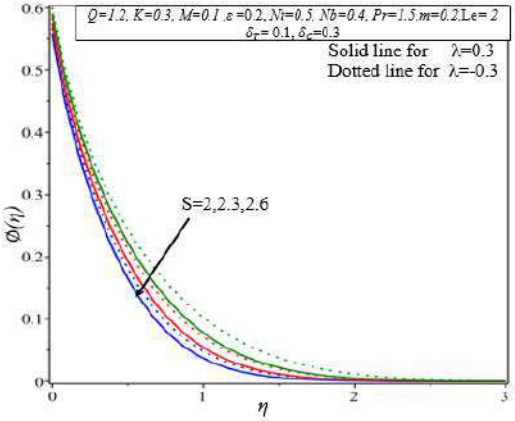

Figure 11. Influence of S on the concentration profile $\phi(\eta)$

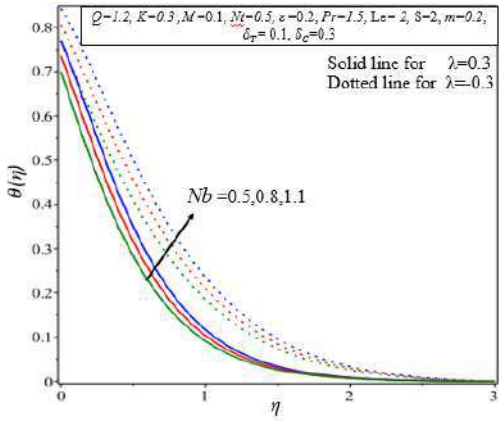

Figure 12. Influence of N_b on the temperature profile $\theta(\eta)$

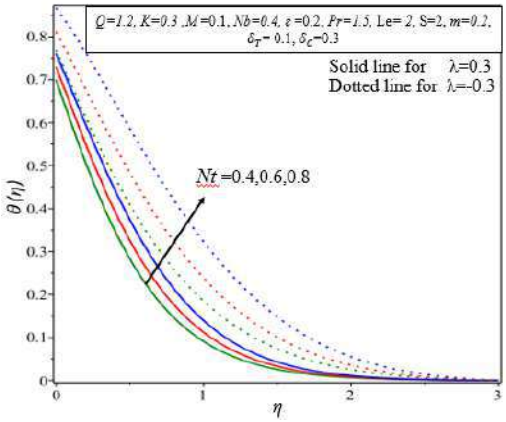

Figure 13. Influence of N_t on the temperature profile $\theta(\eta)$

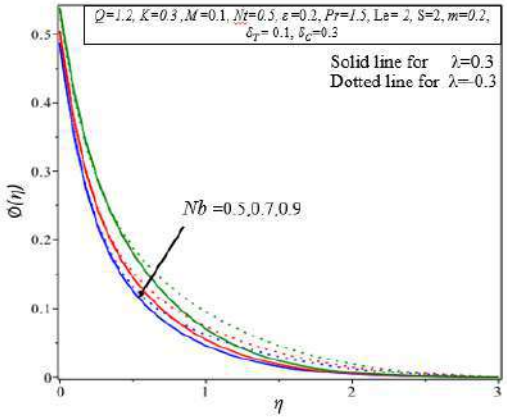

Figure 14. Influence of N_b on the concentration profile $\phi(\eta)$

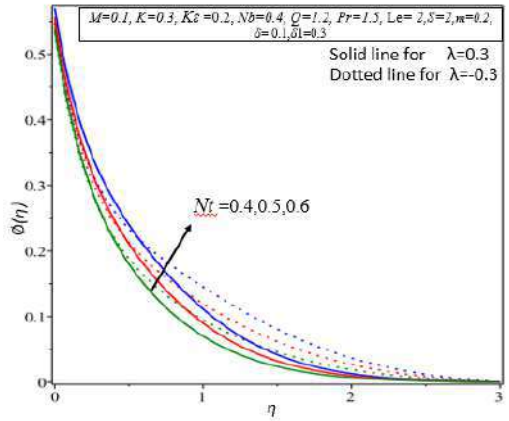

Figure 15. Influence of N_b on the concentration profile $\phi(\eta)$

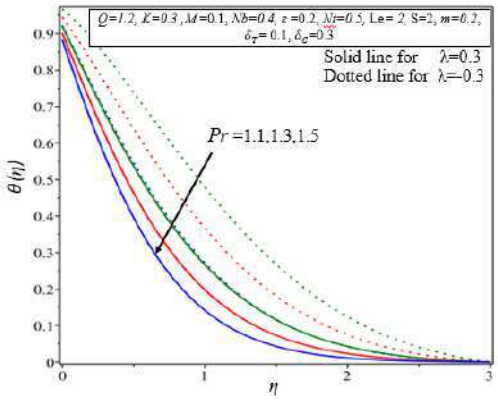

Figure 16. Influence of Pr on the temperature profile $\theta(\eta)$

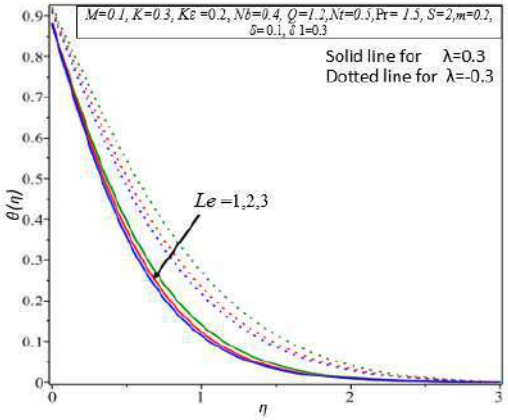

Figure 17. Influence of Le on the temperature profile $\theta(\eta)$

Figure 16 shows the impact of Prandtl number(Pr) on temperature$\theta(\eta)$. Basically, thermal diffusivity of fluids decreases by increasing Prandtl number, which reduces the thickness of thermal boundary layers. As a result, temperature profile along with thermal boundary layer thickness can be seen to decrease as Pr increases.

Figures 17 and 18 demonstrate the impact on temperature and concentration profiles due to variation of Lewis number (*Le*). There is observed that any rise in Lewis number reduces temperature and the concentration profiles and thicknesses of corresponding boundary layers thicknesses for cases of stretching as well as shrinking cases. From Figure 18 it has been observed that concentration profile declines by increase in Lewish number. Since mass diffusivity reduces with increasing Lewish number, a decline in concentration field is caused by a higher mass diffusivity. Therefore, when Le rises, concentration boundary layer thickness reduces.

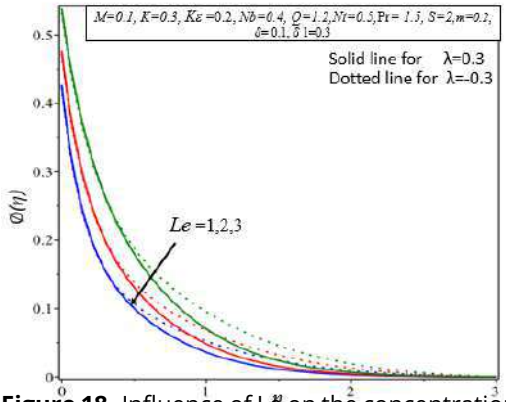

Figure 18. Influence of Le on the concentration profile $\phi(\eta)$

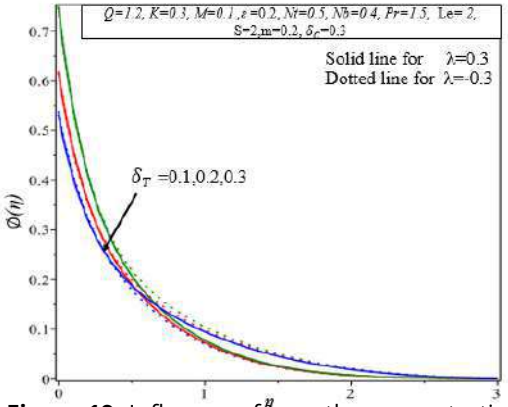

Figure 19. Influence of δ_T on the concentration profile $\phi(\eta)$

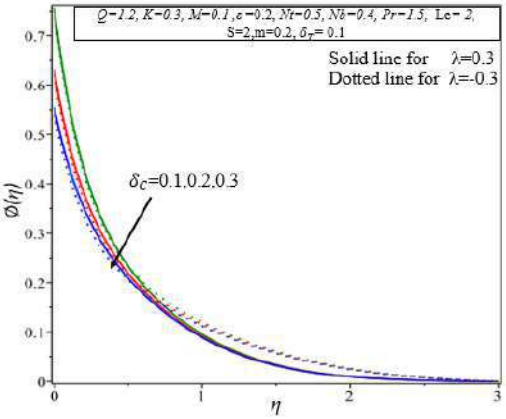

Figure 20. Influence of δ_c on the concentration profile $\phi(\eta)$

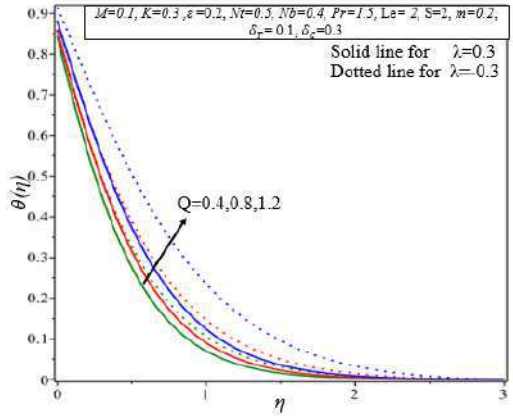

Figure 21. Influence of Q on the temperature profile$\theta(\eta)$

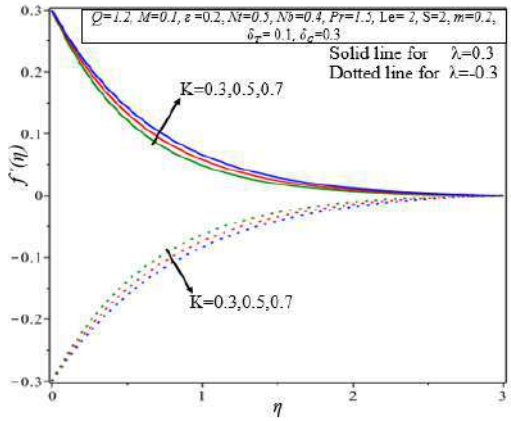

Figure 22. Influence of K on the velocity profile f′(η)

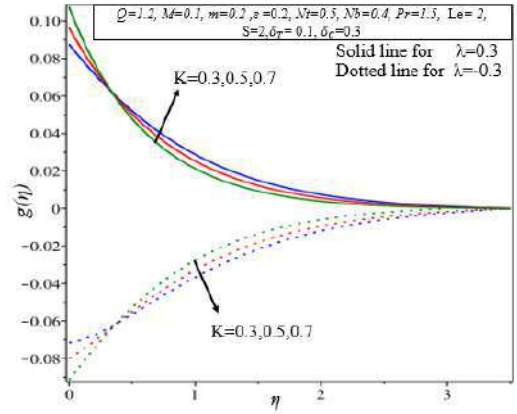

Figure 23. Influence of K on the angular velocity profile g(η)

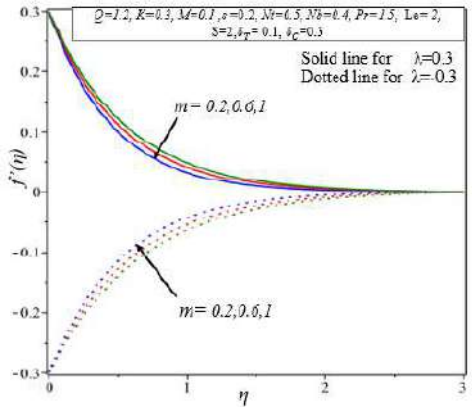

Figure 24. Influence of m on the velocity profile f′(η)

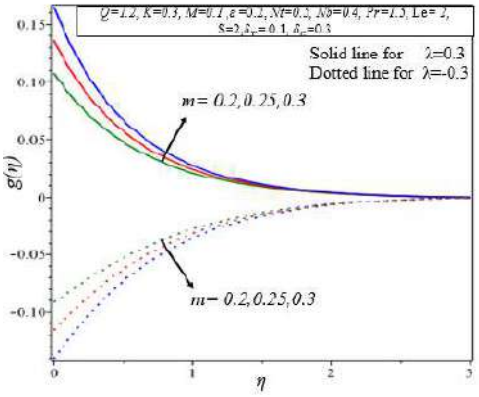

Figure 25. Influence of m on the angular velocity profile g(η)

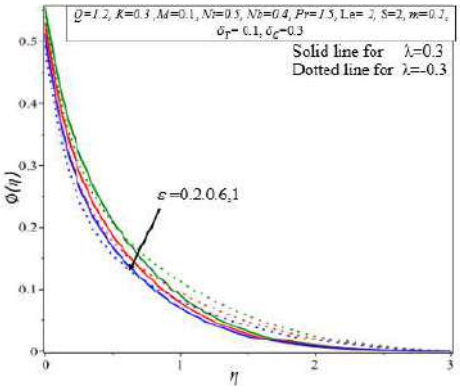

Figure 26. Influence of ϵ on the concentration profile $\phi(\eta)$

In contrast, Figure 19 visually depicts the significant influence exerted on the temperature profile by thermal slip parameter δ_T. There has been observed that temperature profile and its boundary layer thickness declines with increment in the rate of thermal slip parameter δ_T for stretching as well as shrinking cases. Figure 20 demonstrates the impact of concentration slip parameter δ_C on concentration profile. It is seen that when the concentration slip parameter δ_C increases, the concentration profile and its boundary layer thickness is declined for both cases of surfaces stretching and shrinking. The variation of nanofluid temperature profile $\theta(\eta)$ for various values of the heat sink/source parameter (Q)is inspected in Figure 21. Additionally, it has been shown that raising the heat source/sink parameter causes thermal boundary layer thickness to decrease, which enhances temperature profiles. Figures 22-23 demonstrate impacts on the velocity f′(η) and angular velocity profile g(η) of several values of micro material parameter K.There is observed the velocity profile along their boundary layer thickness are increasing with increase in rate of the micro material parameter K for stretching and shrinking cases. While at the start angular velocity of micropolar nanofluid decreases but after a point it increases throughout the flow. Figures 24-25 show the variation of m on the velocity f′(η)and angular velocity profile g(η). The Figure 24 shows that the velocity profile along the boundary layers thickness is decreasing with rise in the m for stretching as well as shrinking cases while angular velocity profile along its boundary layers thickness is increasing with increase in m for stretching and the shrinking cases that is shown in Figure 25. Figure 26 depicts the impact of ϵ on the nanoparticles concentration $\phi(\eta)$.The nanoparticles concentration and concentration boundary

6 Conclusion

The present investigation is an attempt to analyze MHD flow and heat transfer of the micropolar nanofluid over a stretching/shrinking parameter in regard of their significance in the heat transfer procedure in industrial and cooling systems. The equations are constructed by using Buongiorno model with addition of magnetic, heat ource/sink, chemical reaction and slip parameters. The shooting technique is used to detect the influence of various used parameters numerically. The main finding observed during study are:

1. The skin friction and the drag force are decreasing for $\lambda > 0$ and increasing for $\lambda < 0$ when rate of the suction is increased.
2. The heat transfer and concentration rates are increasing for both $\lambda > 0$ and $\lambda < 0$ with increase in suction parameter S.

3. The velocity profiles of the micropolar nanofluid declines with increase in the magnetic parameter M and the suction parameter S, while it rises by increase in stretching parameter λ and micro-material parameter K.
4. The angular velocity profile rises with rise in M and K, but, it declines by rise in S.
5. Temperature of micropolar nanofluid enhances with increase in Q, Nt and Nb, but it decreases due to increase in the δT, Pr and S.
6. The concentration profiles decrease by increase in δC, ϵ, Nb and Le, while it increases for increase in the Nt.

7 Author Contributions

Sanjay Kumar:Conceptualization, Methodology, Software **Asif Ali Shaikh**:Data curation, Writing- Original draft preparation,**Hazoor Bux Lanjwani**:Visualization, Software, Validation, Investigation **Syed Feroz Shah**:Writing- Reviewing and Editing Supervision

8 Compliance with Ethical Standards

It is declare that all authors don't have any conflict of interest. It is also declare that this article does not contain any studies with human participants or animals performed by any of the authors. Furthermore, informed consent was obtained from all individual participants included in the study. harvard style

References

[1] Abbas, N., Rehman, K. U., Shatanawi, W. and Al-Eid, A. A. [2022], 'Theoretical study of non-newtonian micropolar nanofluid flow over an exponentially stretching surface with free stream velocity', *Advances in Mechanical Engineering* **14**(7), 16878132221107790.

[2] Abbas, N. and Shatanawi, W. [2022], 'Theoretical survey of time-dependent micropolar nanofluid flow over a linear curved stretching surface', *Symmetry* **14**(8), 1629.

[3] Abdal, S., Alhumade, H., Siddique, I., Alam, M. M., Ahmad, I. and Hussain, S. [2021], 'Radiation and multiple slip effects on magnetohydrodynamic bioconvection flow of micropolar based nanofluid over a stretching surface', *Applied Sciences* **11**(11), 5136.

[4] Afify, A. A. [2017], 'The influence of slip boundary condition on casson nanofluid flow over a stretching sheet in the presence of viscous dissipation and chemical reaction', *Mathematical Problems in Engineering* **2017**.

[5] Amjad, M., Zehra, I., Nadeem, S. and Abbas, N. [2021], 'Thermal analysis of casson micropolar nanofluid flow over a permeable curved stretching surface under the stagnation region', *Journal of Thermal Analysis and Calorimetry* **143**, 2485–2497.

[6] Anwar, M., Shafie, S., Hayat, T., Shehzad, S. and Salleh, M. Z. [2017], 'Numerical study for mhd stagnation-point flow of a micropolar nanofluid towards a stretching sheet', *Journal of the Brazilian Society of Mechanical Sciences and Engineering* **39**, 89–100.

[7] Aurangzaib, A., Kasim, A., Mohammad, N., Shafie, S. et al. [2013], 'Unsteady mhd mixed convection flow with heat and mass transfer over a vertical plate in a micropolar fluid-saturated porous medium', *Journal of Applied Science and Engineering* **16**(2), 141–150.

[8] Bhatti, M. M., Doranehgard, M. H. and Ellahi, R. [2022], 'Electro-magneto-hydrodynamic eyring-powell fluid flow through micro-parallel plates with heat transfer and non-darcian effects', *Mathematical Methods in the Applied Sciences* .

[9] Chamkha, A. J. and Aly, A. [2010], 'Mhd free convection flow of a nanofluid past a vertical plate in the presence of heat generation or absorption effects', *Chemical Engineering Communications* **198**(3), 425–441.

[10] Choi, S. U. and Eastman, J. A. [1995], Enhancing thermal conductivity of fluids with nanoparticles, Technical report, Argonne National Lab.(ANL), Argonne, IL (United States).

[11] Das, K. [2012], 'Slip effects on heat and mass transfer in mhd micropolar fluid flow over an inclined plate with thermal radiation and chemical reaction', *International Journal for Numerical Methods in Fluids* **70**(1), 96–113.

[12] Dero, S., Rohni, A. M. and Saaban, A. [2019], 'Mhd micropolar nanofluid flow over an exponentially stretching/shrinking surface: Triple solutions', *Journal of Advanced Research in Fluid Mechanics and Thermal Sciences* **56**(2), 165–174.

[13] Eringen, A. C. [1964], 'Simple microfluids', *International Journal of Engineering Science* **2**(2), 205–217.

[14] Hamad, M., Pop, I. and Ismail, A. M. [2011], 'Magnetic field effects on free convection flow of a nanofluid past a vertical semi-infinite flat plate', *Nonlinear Analysis: Real World Applications* **12**(3), 1338–1346.

[15] Ishak, A., Nazar, R. and Pop, I. [2008], 'Heat transfer over a stretching surface with variable heat flux in micropolar fluids', *Physics Letters A* **372**(5), 559–561.

[16] Kasaeian, A., Daneshazarian, R., Mahian, O., Kolsi, L., Chamkha, A. J., Wongwises, S. and Pop, I. [2017], 'Nanofluid flow and heat transfer in porous media: a review of the latest developments', *International Journal of Heat and Mass Transfer* **107**, 778–791.

[17] Khaskheli, M. A., Memon, K. N., Sheikh, A. H., Siddiqui, A. M. and Shah, S. F. [2020], 'Tank drainage for an electrically conducting newtonian fluid with the use of the bessel function', *Eng. Technol. Appl. Sci. Res* **10**(2).

[18] Krajnik, P., Pusavec, F. and Rashid, A. [2011], Nanofluids: properties, applications and sustainability aspects in materials processing technologies, *in* 'Advances in Sustainable Manufacturing: Proceedings of the 8th Global Conference on Sustainable Manufacturing', Springer, pp. 107–113.

[19] Kuznetsov, A. and Nield, D. [2010], 'Natural convective boundary-layer flow of a nanofluid past a vertical plate', *International Journal of Thermal Sciences* **49**(2), 243–247.

[20] Lanjwani, H. B., Chandio, M. S., Anwar, M. I., Al-Johani, A. S., Khan, I., Alam, M. et al. [2022], 'Triple solutions with stability analysis of mhd mixed convection flow of micropolar nanofluid with radiation effect', *Journal of Nanomaterials* **2022**.

[21] Lanjwani, H. B., Chandio, M. S., Malik, K. and Shaikh, M. M. [2022], 'Stability analysis of boundary layer flow and heat transfer of fe2o3 and fe-water base nanofluid over a stretching/shrinking sheet with radiation effect', *Engineering, Technology & Applied Science Research* **12**(1), 8114–8122.

[22] Lanjwani, H., Chandio, M., Anwar, M., Shehzad, S. and Izadi, M. [2021], 'Dual solutions of time-dependent magnetohydrodynamic stagnation point boundary layer micropolar nanofluid flow over shrinking/stretching surface', *Applied Mathematics and Mechanics* **42**(7), 1013–1028.

[23] Lukaszewicz, G. [1999*a*], *Micropolar fluids: theory and applications*, Springer Science & Business Media.

[24] Lukaszewicz, G. [1999*b*], *Micropolar fluids: theory and applications*, Springer Science & Business Media.

[25] Meade, D. B., Haran, B. S. and White, R. E. [1996], 'The shooting technique for the solution of two-point boundary value problems', *Maple Technical Newsletter* **3**(1), 1–8.

[26] Memon, K., Islam, S., Siddiqui, A., Khan, S. A., Zafar, N. A. and Akram, M. [2014], 'Lift and drainage of electrically conducting power law fluid on a vertical cylinder', *Applied Mathematics & Information Sciences* **8**(1), 45.

[27] Memon, K. N., Alam, M. K., Baili, J., Nawaz, Z., Shiekh, A. H. and Ahmad, H. [2021], 'Analytical solution of tank drainage flow for electrically conducting newtonian fluid', *Thermal Science* **25**(Spec. issue 2), 433–439.

[28] Nazar, R., Jaradat, M., Arifin, N. and Pop, I. [2011], 'Stagnation-point flow past a shrinking sheet in a nanofluid', *Open Physics* **9**(5), 1195–1202.

[29] Sadiq, K., Jarad, F., Siddique, I. and Ali, B. [2021], 'Soret and radiation effects on mixture of ethylene glycol-water (50%-50%) based maxwell nanofluid flow in an upright channel', *Complexity* **2021**, 1–12.

[30] Srinivasacharya, D. and Bindu, K. H. [2016*a*], 'Entropy generation in a micropolar fluid flow through an inclined channel', *Alexandria engineering journal* **55**(2), 973–982.

[31] Srinivasacharya, D. and Bindu, K. H. [2016*b*], 'Entropy generation in a micropolar fluid flow through an inclined channel', *Alexandria engineering journal* **55**(2), 973–982.